MEASUREMENT OF A WIDE RANGE OF INTRACELLULAR SODIUM CONCENTRATIONS IN ERYTHROCYTES BY ^{23}NA NUCLEAR MAGNETIC RESONANCE

YVAN BOULANGER,* PATRICK VINAY,‡§ AND MICHEL DESROCHES§
*Institut de Génie Biomédical and ‡Départements de Médecine et de §Physiologie, Université de Montréal, Montréal, Canada H3C 3J7

ABSTRACT The accuracy of the ^{23}Na nuclear magnetic resonance (NMR) method for measuring the sodium concentration in erythrocytes was tested by comparing the NMR results to those obtained by emission-flame photometry. Comparisons were made on aqueous solutions, hemolysates, gels, ghosts, and intact erythrocytes. The intra- and extracellular ^{23}Na NMR signals were distinguished by addition of the dysprosium tripolyphosphate [$Dy(PPP)_2^{7-}$] shift reagent to the extracellular fluid. The intra- and extracellular volumes of ghosts and cells were determined by the isotope dilution method. Our results indicate that >20% of the intracellular signal remains undetected by NMR in ghosts and cells. When the cells are hemolyzed, the amount of NMR-detectable sodium varies depending on the importance of gel formation. In hemolysates prepared by water addition, the NMR and flame photometry results are identical. The loss of signal in ghosts, cells, and undiluted hemolysates is attributed to partial binding of the Na^+ ion to intracellular components, this binding being operative only when these components exist in a gel state. In a second part, ^{31}P NMR was used to monitor the penetration of the shift reagent into the cells during incubation. Our data demonstrate that free Dy^{3+} can slowly accumulate inside the red cell.

INTRODUCTION

The measurement of sodium concentrations in biological fluids by conventional techniques (e.g., flame photometry, atomic absorption) is an invasive procedure requiring the destruction of the fluid analyzed (1). Measurement of cellular sodium concentration with microelectrodes in situ involves a micropuncture and disruption of membrane continuity. In contrast, ^{23}Na NMR allows the noninvasive monitoring of the sodium content in living tissues. The detection of ^{23}Na, with a natural abundance of 100%, can be accomplished relatively easily by nuclear magnetic resonance (NMR) at biological concentrations (5–150 mM). However, the resonances of the intra- and extracellular sodium are overlapping due to the equivalent ionic strength on both sides of the membrane. Early ^{23}Na NMR studies have been unable to differentiate the two compartments (2–5). Recently, the use of membrane-impermeable shift reagents has been introduced, allowing a separation of the intra- and extracellular sodium signals (6–15). The best results for separation and linewidth have been obtained with anionic complexes of dysprosium (6–15) although complexes of thulium are also adequate (12, 15). This technique has been applied to artificial systems such as unilamellar vesicles (10), to cells such as *Saccharomyces cerevisiae* (11, 13) and erythrocytes (7–9), as well as to an isolated organ, the frog skeletal muscle (7).

An early ^{23}Na NMR study on human erythrocytes concluded that all the intracellular sodium was detected in these cells (4), with an average of 92% of the sodium detected. This conclusion was different from the results obtained with other tissues where only 40% of the sodium was observable by NMR (2). In contrast, in a subsequent study on ghosts obtained from pig erythrocytes, a loss in NMR signal intensity corresponding to 5.5% per percent–dry-weight cell was reported (5). This finding was suggestive of significant binding of sodium to intracellular components, maybe to the internal side of the (Na, K)ATPase enzyme. More recently, two limited studies (8, 9) on human erythrocytes have supported the conclusion that all the intracellular sodium is NMR visible. Moreover, several important parameters have been neglected in the studies mentioned above (cell sedimentation, hematocrit, gel formation). Furthermore, it must be realized that in both man and pig erythrocytes, the intracellular sodium concentration is low (<15 mM) compared with the extracellular concentration (150 mM) (16). Therefore, the quantitation of intracellular sodium by both conventional means and ^{23}Na NMR is difficult.

We undertook to quantify the sodium content of intact erythrocytes from different species using the paramagnetic shift reagent dysprosium tripolyphosphate, $Dy(PPP)_2^{7-}$, to

Please address all correspondence to Dr. Yvan Boulanger, Institut de Génie Biomédical, Faculté de Médecine, Université de Montréal, Montréal, Québec, Canada H3C 3J7.

distinguish between intra- and extracellular sodium. The species were chosen because their erythrocytes present different sodium contents and (Na, K)ATPase activities. At one extreme, erythrocytes from rat and man possess high (Na, K)ATPase activities and low intracellular sodium concentrations (<15 mM) (16, 17). At the other extreme, dog erythrocytes are devoid of (Na, K)ATPase activity and their intracellular sodium concentration is approximately equivalent to the extracellular sodium concentration (150 mM) (18). Sheep erythrocytes were also used since their sodium contents and ATPase activities are intermediate (16). Furthermore, using erythrocytes from man and dog, we have prepared red-cell ghosts with intracellular sodium concentrations ranging from 10 to 300 mM. Intracellular sodium determinations by NMR and flame photometry were compared, using radioactive markers (^3H_2O and ^{14}C-inulin) to measure the volumes of the intra- and extracellular spaces. Our results indicate that a significant fraction of the intracellular sodium remains undetected by NMR regardless of the intracellular sodium concentration or (Na, K)ATPase activity. When the cells are hemolyzed, however, different results can be obtained depending on the formation of a gel state. The loss in ^{23}Na signal intensity is therefore attributable to the intracellular gel formation.

MATERIALS AND METHODS

Materials

Dysprosium chloride ($DyCl_3$) and dysprosium oxide (Dy_2O_3) were obtained from Aldrich Chemical Co. (Milwaukee, WI). Sodium tripolyphosphate, crystalline fibrinogen and thrombin were purchased from Sigma Chemical Co. (St Louis, MI). Dysprosium oxide was transformed into dysprosium chloride by acidifying an aqueous suspension of dysprosium oxide with concentrated HCl until dissolution occurred. $Dy(PPP)_2^{7-}$ was prepared by titrating dysprosium chloride with sodium tripolyphosphate to obtain a molar ratio 1:2 (19), and then adjusting the pH to 7.4. In some experiments where a low sodium concentration was required in the extracellular fluid (ghost preparations), potassium tripolyphosphate was prepared by cation exchange of sodium tripolyphosphate using a K-loaded ion-exchange resin (AMBERLITE IR-120). Tritiated water (^3H_2O), ^{14}C-inulin, Triton X-100 and scintillation cocktail (AQUASOL) were obtained from New England Nuclear (Boston, MA). Deuterium oxide (^2H_2O) was purchased from Merck, Sharp and Dohme (Pointe-Claire, Canada). Nystatin was obtained as an aqueous suspension from Squibb Canada Inc. (Montreal, Canada). Saponin and sodium hydrosulfite (dithionite) were purchased from Fisher Scientific Co. (Fair Lawn, NJ).

Hemolysates

Heparinized dog or human blood was centrifuged and washed several times with a 5% D-glucose solution. The cell pellet was then hemolyzed by addition of water (2:1 vol/vol) and homogenized. The sodium content of the hemolysates was varied between 20 and 200 mM by addition of small volumes of a concentrated solution of sodium chloride (1 M). In some experiments, KCl (100 or 400 mM) was added to the hemolysates. In another series of experiments, hemolysates were prepared by adding either water (2:1 vol/vol) or a mixture of Triton X-100 and saponin (1:8 vol/vol) to dog erythrocyte suspensions in 5% D-glucose with hematocrit values ranging from 10 to 60%.

Gels

Experiments were performed on two types of gel. An agar gel was prepared by dissolving 2% agar wt/vol in sodium chloride solutions at concentrations ranging from 20 to 160 mM. The samples were prepared directly in the NMR tube and flame photometry measurements were made before the agar addition. To study biologically-relevant gels, 2 ml fibrinogen solutions were prepared in 0.1 M sodium phosphate buffer, pH 7.4, and 50 μl thrombin solution (100 units/ml) were added. The ^{23}Na NMR spectra were recorded before and after the addition of thrombin. The flame photometry measurements were performed before coagulation with thrombin.

Erythrocyte Ghosts

Heparinized fresh dog or human blood was washed and resuspended in a 5% D-glucose solution to obtain an hematocrit value of 50%. The blood was divided into individual samples and centrifuged. The supernatant was decanted and the cell pellet weighted. The erythrocytes were resuspended to obtain a hematocrit value of 5% with NaCl solutions of different concentrations containing 5 mM $Dy(PPP)_2^{7-}$, 68mM sucrose, 100–400 mM KCl, and 10 mM Tris [tris(hydroxymethyl)aminomethane], at pH 7.4 (20). The dysprosium complex was added to shift the extracellular sodium signal upfield by ~1,000 Hz (the shift varies with the sodium concentration). Nystatin was added to obtain a final concentration of 1 mg/ml. The samples were incubated at 4°C for 24 h with slow agitation. After this period, the ghost suspensions were centrifuged for 15 min at 2,800 rpm and the supernatant was removed and kept aside. The cell pellet was weighted and a suspension of hematocrit 50% was prepared by reintroducing adequate amounts of the same supernatant. These samples were put in 10 mm NMR tubes and their ^{23}Na NMR spectra were recorded.

Following the NMR measurement, the aqueous volume markers ^{14}C-inulin (160,000 DPM/ml) and ^3H_2O (40,000 DPM/ml) were added to the ghost suspensions. The ghosts were incubated for 10 min at 4°C, centrifuged, and the supernatant removed. Trichloroacetic acid (10% wt/vol) was added to the supernatant (vol/vol) to denature any residual protein (especially colored hemoglobin). The ^{3}H and ^{14}C counts and the sodium concentrations were measured on the trichloroacetic acid filtrate. The cell pellet was weighted, 10% trichloroacetic acid was added (vol/vol) and the sample was centrifuged. The acid filtrate was used as above. All counts were measured on an LKB scintillation counter (Fisher Scientific Co., Fair Lawn, NJ) using a dual isotope program. Small amounts of chloroform were added to the scintillation cocktail in order to obtain optimal quenching for dual isotope determination. Quantitation of both isotopes in DPM/ml was obtained by the external standard ratio procedure. Sodium and potassium concentrations were determined by emission flame photometry using an IL 343 instrument (Instrument Laboratory, Lexington, MA) and intracellular sodium concentrations measured by NMR and photometry were compared.

The prolonged equilibration time allowed the intra- and extracellular cations to equilibrate in the presence of nystatin. In accord, the sodium concentration calculated for the intracellular compartment was identical to that measured in the extracellular fluid (man: intercept $a = -4.02$, slope $b = 0.986$, correlation coefficient $r^2 = 0.993$; dog: $a = 6.05$, $b = 0.934$, $r^2 = 0.962$). In this case, the agreement between intra- and extracellular measurements indicates that our methods for estimation of both intracellular sodium content and aqueous volume are adequate.

Erythrocytes

Heparinized fresh blood was obtained from different species (man, rat, sheep, and dog), washed several times and resuspended in an isosmotic solution prepared by mixing various amounts of 5% D-glucose and 0.9% NaCl. $Dy(PPP)_2^{7-}$ was added to the suspension in order to obtain a 5 mM final concentration. The blood samples were used directly for NMR, after which the procedure described for measuring intracellular sodium and potassium in erythrocyte ghosts was performed.

NMR Measurements

^{23}Na and ^{31}P NMR spectra were acquired at 105.6 and 162.0 MHz, respectively, on a spectrometer (WH-400; Bruker Instruments, Hannover, Federal Republic of Germany). For ^{23}Na NMR, blood samples were placed in a 10 mm o.d. NMR tube into which was inserted a 4 mm o.d. coaxial tube containing 0.6 M NaCl, 50 mM $DyCl_3$ in 99.8% ^2H_2O. $DyCl_3$ shifted the sodium signal in the coaxial compartment downfield by 1,000 Hz (i.e., in the opposite direction of the $Dy(PPP)_2^{7-}$ shift). The coaxial solution was used as a field/frequency lock and as a quantitative external standard. The sample was rotated at 20 rpm and 48–200 accumulations with a recycle time of 0.6 s were recorded at 37°C. The estimation of the sodium concentration was obtained from a calibration curve established with NaCl standards (30, 60, 90, 120, and 150 mM) using the following procedure. First, the peak area of the ^{23}Na signal of each NaCl standard was divided by that of the fixed external standard placed in the inner coaxial tube. The resulting ratio (I_x/I_{std}) was plotted as a function of the sodium concentration in each standard as determined by emission-flame photometry. This function was a straight line ($r^2 = 0.999$) in the concentration range 0–200 mM and beyond. For ^{31}P NMR, the same sample configuration was used, the coaxial sample serving as field/frequency lock. The spectra were acquired at 37°C using a recycle time of 1.41 s, a pulse angle of 90° (60 μs) and 1,000–2,000 accumulations.

Membrane Permeability to Dysprosium

The presence of dysprosium in the environment of phosphate-containing metabolites such as ATP, ADP, inorganic phosphate, and phosphocreatine causes a sizable broadening and shift of their ^{31}P NMR resonances. When dysprosium is added to the extracellular compartment, its membrane permeability can be monitored by observing the ^{31}P NMR spectrum, since the phosphate metabolites are solely intracellular. Human erythrocyte samples were then prepared as described above and their ^{31}P spectrum was recorded as a function of incubation time at 37°C.

To monitor the possible effect of the deoxyhemoglobin formation on the NMR linewidths during these experiments, the spectra of human erythrocyte samples were recorded before and after reduction of all oxyhemoglobin to deoxyhemoglobin by addition of adequate amounts of sodium dithionite (4.9 mg/ml sample).

Calculation of Intracellular Sodium Concentration Using Photometry

The intracellular aqueous volume V_i of erythrocytes or ghosts was calculated from ^3H_2O and ^{14}C-inulin spaces, which measure, respectively, the total aqueous volume (V_t) and the extracellular aqueous volume (V_e)

$$V_i = V_t - V_e. \tag{1}$$

These volumes were calculated as follows. First, the ^3H and ^{14}C concentrations in disintegrations per minute per milliliter were determined in the supernatant (s) and referred to as T_{sv} and C_{sv}, respectively

$$T_{sv} = T_s F_d / V_{sr}; \qquad C_{sv} = C_s F_d / V_{sr}, \tag{2}$$

where T_s and C_s are, respectively, the ^3H and ^{14}C dpm in the same of supernatant filtrate, F_d is the dilution factor, i.e., the ratio of the volumes after and before trichloroacetic acid deproteinization and V_{sr} is the sample volume used for radioactivity counting. In the cell pellet, the volumes corresponding to the ^3H and ^{14}C distribution, V_t and V_e, are given by

$$V_t = T_p V_p / T_{sv} V_{pr}; \qquad V_e = C_p V_p / C_{sv} V_{pr}, \tag{3}$$

where T_p and C_p are the ^3H and ^{14}C dpm in the cell filtrate, V_p is the total volume of the pellet after trichloroacetic acid addition and V_{pr} is the volume used for radioactivity counting. The intracellular volume V_i corresponds to the difference between the ^3H and ^{14}C distribution volumes (Eq. 1), and the sodium concentration in the cell $[Na_i]$ is given by

$$[Na_i] = ([Na_p]V_p - [Na_s]V_e F_d)/V_i, \tag{4}$$

$[Na_p]$ and $[Na_s]$ being the sodium concentrations in the cell pellet and the supernatant filtrates, respectively. In ghosts and under our conditions, the intracellular sodium can also be obtained by measuring the extracellular sodium. The good agreement between both measurements confirmed the validity of the above procedure in red cells.

Calculation of Intracellular Sodium Concentration Using ^{23}Na NMR

For the NMR experiments, the sodium concentrations in the intracellular space $[Na_i]'$ and in the extracellular fluid $[Na_e]'$ were directly determined from a comparison of the ^{23}Na NMR signal area to the calibration curve. Knowing the sodium concentration of the supernatant as determined by flame photometry, the hematocrit Hte of the NMR sample can be calculated

$$Hte = [1 - ([Na_e]'/[Na_s])] \times 100. \tag{5}$$

The intracellular sodium concentration can then be calculated using this hematocrit and the volume fraction of water in the cells, F

$$[Na_i] = ([Na_i]'/Hte\ F) \times 100. \tag{6}$$

F was calculated for each sample from the intracellular volume of water measured by the isotope dilution method and the weight of the red cells.

Any change of hematocrit in the critical segment of the NMR tube during the measurements would be automatically taken into account since the hematocrit is directly and simultaneously determined by NMR for each sample (Eq. 5). The quality of the signal-to-noise ratio obtained in our spectra (Fig. 1) precludes any significant uncertainty in the integration of the ^{23}Na signals, except at very low concentrations (<5 mM). Thus, the sensitivity of the ^{23}Na nucleus ensures the accuracy of the method at existing biological concentrations.

RESULTS AND DISCUSSION

Detection of Sodium in the Intracellular Space by ^{23}Na NMR

^{23}Na NMR spectra obtained from dog erythrocytes suspended in saline buffer with different $Dy(PPP)_2^{7-}$ concentrations (0–10 mM) are presented in Fig. 1. The invariant downfield resonance in all spectra is due to the coaxial standard sample consisting of a NaCl-$DyCl_3$ solution in ^2H_2O. Fig. 1 shows the spectrum obtained in the absence of $Dy(PPP)_2^{7-}$ where the signals of the intracellular and extracellular sodium ions are overlapping. Upon progressive addition of $Dy(PPP)_2^{7-}$, while keeping the extracellular sodium concentration constant (Fig. 1 *b–g*), an upfield shift of the extracellular signal is observed. The shift is linearly dependent on the $Dy(PPP)_2^{7-}$ concentration, as illustrated in Fig. 2, which is consistent with a chemical equilibrium interaction of the Na^+ ion with the dysprosium complex (19).

No loss in the intensity of both the intra- and extracellular ^{23}Na signals is detected upon addition of $Dy(PPP)_2^{7-}$. This is ascertained by the total surface measured, $Na_i + Na_e$, which remains constant between 0 and 7 mM

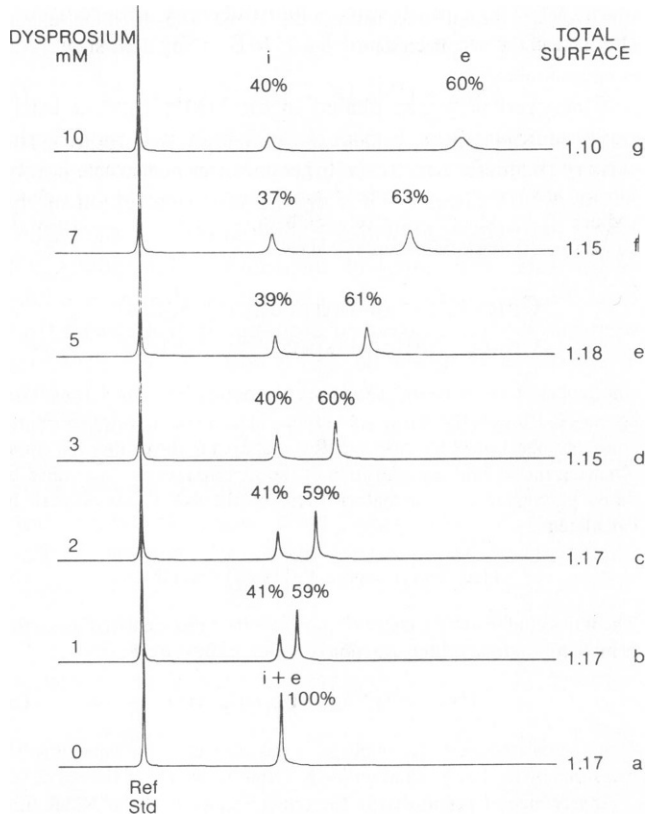

FIGURE 1 ^{23}Na NMR spectra (105.6 MHz) of a suspension of dog erythrocytes in a 0.9% NaCl solution at pH 7.4 containing (*a*) 0, (*b*) 1, (*c*) 2, (*d*) 3, (*e*) 5, (*f*) 7, and (*g*) 10 mM dysprosium tripolyphosphate. Each spectrum was acquired at 37°C with a 60 μs pulse length (90°), a spectral width of 5 kHz, a recycle time of 0.6 s, and 48 accumulations.

$Dy(PPP)_2^{7-}$, together with the constant 60%:40% distribution of the signals originating from the extra- and intracellular sodium. This indicates that the interaction between the sodium ions and the shift reagent complex is too weak to give rise to any quadrupolar effect that would reduce the

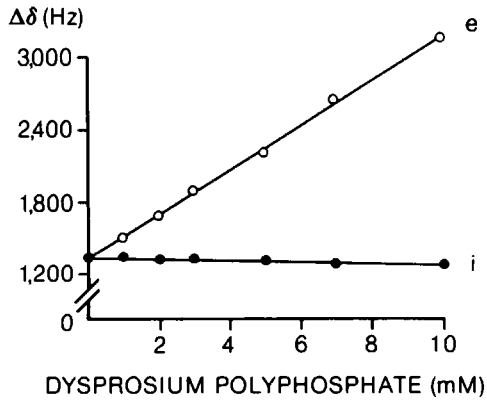

FIGURE 2 Graph of the chemical shift difference (Δδ) between the intra- (*i*) and extra- (*e*) cellular ^{23}Na resonances of a dog erythrocyte suspension and the external standard (0.6 M NaCl, 50 mM $DyCl_3$ in ^2H_2O) as a function of the dysprosium tripolyphosphate concentration for the spectra shown in Fig. 1.

detectable signal intensity (2). Nevertheless, some line broadening of the signals of both the intra- and extracellular sodium is observed. The presence of dysprosium in the extracellular fluid, besides altering the chemical shift, can enhance the relaxation rate of the ^{23}Na (21) and cause this line broadening. The origin of the broadening of the intracellular signal is less clear. It may be attributed to a local change in magnetic susceptibility due to the external paramagnetic agent (22) or to the penetration of small amounts of dysprosium ion into the cell. This latter possibility is suggested by the small but progressive downfield shift observed for intracellular sodium when increasing quantities of $Dy(PPP)_2^{7-}$ are added to the extracellular solution (Fig. 2). Note that the shift is in the opposite direction to that observed in the extracellular fluid, indicating that the tripolyphosphate ligand probably does not enter the cell or is locally metabolized. Definite evidence for the slow penetration of dysprosium into the cell with prolonged incubation is given below.

Gels

For sodium concentrations ranging from 20 to 160 mM, NMR readings were identical in aqueous solutions and 2% agar gels. In contrast, using purified fibrinogen solutions, the NMR signals were significantly decreased (−10%) following thrombin addition and gel formation, indicating that the physical state of the environment is capable of modifying interactions between sodium and the surrounding proteins. Further observations of this phenomenon on red cell hemolysates are presented below.

Erythrocyte Hemolysates

Fig. 3 presents the relationship between the sodium concentrations as determined by ^{23}Na NMR and flame photometry on red-cell hemolysates of dog and man. When the hemolysates were prepared by adding water to the cell pellet in the volume ratio 2:1 with supplementation of various amounts of sodium (0–150 mM) and potassium chloride (0–100 mM), the NMR and flame photometry results were in perfect agreement ($a = -1.40$; $b = 1.01$; $r^2 = 0.992$; Fig. 3). When the hemolysates were prepared without the addition of water, different results were obtained as discussed below (Fig. 6).

Note that for solutions with a high nonaqueous content, care must be taken to compare measurements determined by flame photometry on the nondeproteinized solutions or to correct for the nonaqueous volume in order to obtain comparable conditions for photometry and NMR measurements.

Erythrocyte Ghosts and Cells

Fig. 4 shows a comparison of intracellular sodium studied over a wide range of concentrations in ghosts prepared from dog and man erythrocytes as determined by flame photometry and ^{23}Na NMR. Almost all the points in Fig. 4

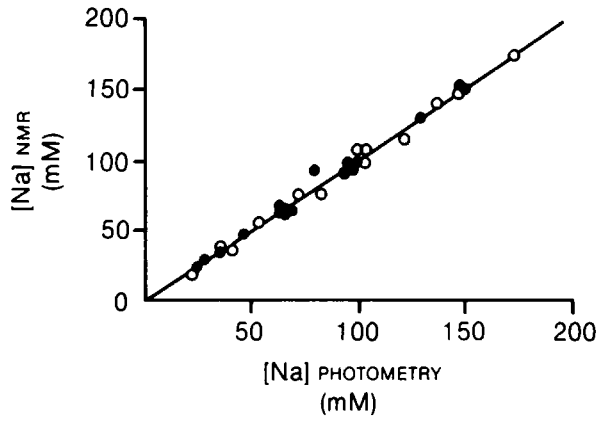

FIGURE 3 Correlation between the sodium concentration of dog (O) and man (●) hemolysates determined by ^{23}Na NMR and emission flame photometry. The identity line is shown in the graph. (n = 36, a = −1.4, b = 1.01, r^2 = 0.992.)

fall below the identity line indicating that a significant part of the intracellular sodium is not detected by NMR. On the average, 78.9 ± 12.6% of the Na_i measured by flame photometry is seen by NMR, suggesting that part of the sodium is sufficiently immobilized to experience a line-broadening quadrupolar interaction.

That the difference between both readings is indeed due to a partial NMR visibility of intracellular sodium is suggested by the following considerations: (*a*) the calculation of the intracellular sodium concentrations ($[Na_i]$) by both flame photometry and ^{23}Na NMR depends on the estimation of the intracellular volume by the isotope dilution method (^{14}C-inulin and ^3H_2O radioactive markers). Any error in the determination of the compartment volumes would influence equally the results of both methods. (*b*) Furthermore, the identity of intra- and extracellular sodium concentrations was established by photometry in ghosts when both the intra- and extracellular compartments were at equilibrium, while different apparent concentrations were measured by NMR using the same cell suspensions.

When red cells are placed in an NMR tube, a fairly rapid sedimentation is occurring, which will modify the ratio of the intra- to extracellular volumes across the height of the NMR sample. Thus, in the sensitive region of the NMR observing coil, which is located towards the bottom of the tube, the signal of the intracellular sodium will increase with time at the expense of the extracellular sodium. We have measured a change in hematocrit from 45 to 60% in 15 min under our conditions (our measuring time was 3–5 min). It was thus necessary to know the hematocrit at the time of the NMR measurement. This value was calculated from the extracellular volume estimated from the extracellular sodium content as determined by ^{23}Na NMR (Eq. 5) and the extracellular sodium concentration as measured by flame photometry. This calculation relies on the fact that the entire extracellular sodium is NMR-visible, which was confirmed by ^{23}Na NMR measurements on solutions and hemolysates.

In Fig. 5, the correlation between the sodium concentra-

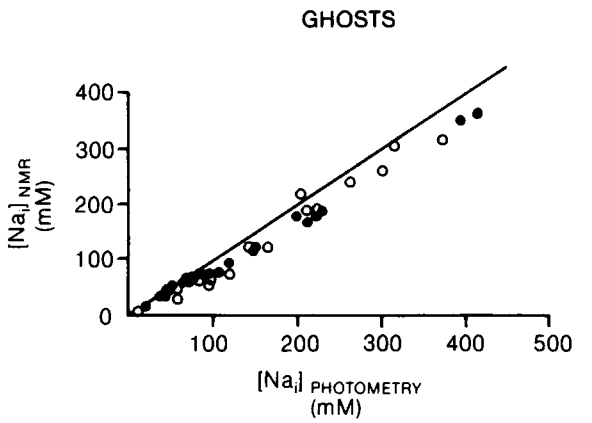

FIGURE 4 Correlation between the intracellular sodium concentrations as determined by ^{23}Na NMR ($[Na_i]_{nmr}$) and emission flame photometry ($[Na_i]_{photometry}$) in erythrocyte ghosts prepared with nystatin using dog (O) (n = 22) and man (●) (n = 29) red cells. Ghosts were suspended in 10 mM Tris, 68 mM sucrose, 100 mM KCl, 5 mM $Dy(PPP)_2^{7-}$ and NaCl solutions at pH 7.4. The identity line is traced on the graph.

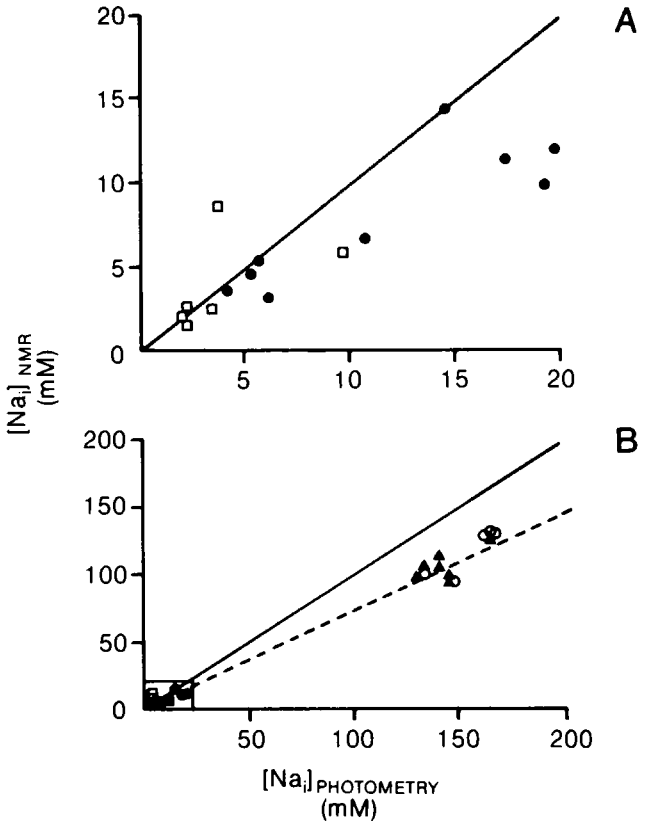

FIGURE 5 Correlation between the intracellular sodium concentrations as determined by ^{23}Na NMR and emission flame photometry in erythrocyte suspensions of dog (O) (n = 5), man (●) (n = 9), rat (□) (n = 6), and sheep (△) (n = 9). The suspension medium consisted of isoosmotic solutions of 10 mM Tris, 68 mM sucrose, 100 mM KCl, and 5 mM $Dy(PPP)_2^{7-}$ at pH 7.4. Appropriate amounts of 0.9% NaCl and 5% D-glucose were added as needed. The identity line is traced on the graph. (n = 29, a = −0.097, b = 0.743, r^2 = 0.998.)

tions determined by ^{23}Na NMR and emission flame photometry is given for intact erythrocytes from different species (dog, man, rat and sheep) possessing different intracellular sodium concentrations and (Na,K)ATPase activities. The relationship between the two measurements is similar to that observed for erythrocyte ghosts (Fig. 4), i.e., only 75.3 ± 14.5% of the sodium is NMR visible. The percentage of sodium detected by NMR is similar whether the erythrocytes possess low (sheep), high (rat, man), or no (dog) (Na, K) ATPase activity. Thus, the intracellular sodium binding sites of this enzyme do not appear to be responsible for the loss in ^{23}Na NMR signal.

The results of Figs. 3–5 are confirmed by a direct comparison of the NMR signals obtained from dog erythrocytes suspended in sodium-free 5% D-glucose before and after hemolysis by addition of either water or a Triton X-100 saponin mixture (Fig. 6). Curve A in Fig. 6 corresponds to the hemolysates prepared by water dilution and is 25% higher than curve B, which corresponds to intact erythrocytes. When hemolysates are prepared by addition of a small quantity of Triton X-100 saponin, curves C and D of Fig. 6 are obtained, showing a loss of signal intensity that is more pronounced at higher hematocrit values. In these samples, gel formation was clearly observable and was increasing with the hematocrit as well as with time (2 min vs. 1 h). We believe that these results provide the explanation for the loss of signal intensity observed in ghosts and intact cells, since it is known that the cytoplasm exists in a gel state. Note that identical sodium readings can be fortuitously observed (e.g., at hematocrits of 20 and 40% in Fig. 6) when the loss of signal in hemolysates due to gel formation happens to be equal to that seen in intact cells. An immobilization of the sodium ion in gels would give rise to a variable quadrupolar interaction, depending on the density of the gel state, and would cause line broadening.

The effect of the quadrupolar interaction on the NMR spectra of ions has been analyzed in detail (2, 23, 24). In conditions where a spin-3/2 ion is tightly bound or in fast exchange between free and bound states, the transverse relaxation time T_2 of the ion is described as the sum of two exponentials (23). These exponentials correspond to the wide and narrow signals in the Fourier-transformed spectrum whose intensities are in the ratio 6:4. The wide signal is usually indistinguishable from the baseline, and a maximal intensity loss of 60% is expected. Moreover, the lineshape of the narrow signal is affected by the underlying signal. We have compared the lineshapes of the signals of the intracellular sodium in erythrocytes to the signals in solution by measuring the ratio of the line width at one-eighth of the height to the line width at half height. The intracellular sodium signals had ratios 15–20% higher than the solution signals. These measurements are an additional indication that the intracellular Na^+ ions experience a quadrupolar interaction due to their binding to intracellular components. However, this interaction does not involve the totality of the ions since a signal loss of only 20% is measured, well below the 60% loss expected for complete interaction and reported in most other tissues studied by this technique (2, 24).

Comparison with Other Studies

Our results are in disagreement with an early continuous-wave ^{23}Na NMR study on human erythrocytes that con-

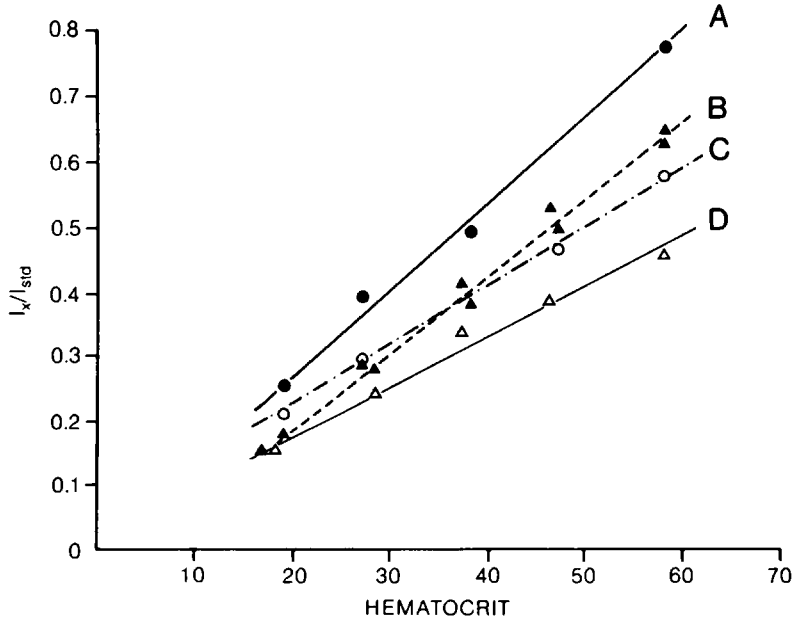

FIGURE 6 Variation of the ^{23}Na NMR signal intensity as a function of the hematocrit for dog erythrocyte suspensions in 5% D-glucose before hemolysis (curve *B*) and after hemolysis by addition of water (curve *A*) or a Triton X-100 saponin mixture (curve *C*, 2 min after hemolysis; curve *D*, 1 h after hemolysis).

cluded that all the sodium could be detected, based on a comparison of the NMR signals of erythrocytes suspended in sodium-free buffer before and after hemolysis by freeze thawing as well as comparison of flame photometry and NMR measurements on hemolysates (4): the intensity of the ^{23}Na NMR signal in intact cells was 98% of that present in the same samples after freeze-thawing hemolysis. It is likely, considering our results described in Fig. 6, that in this study a gel was formed in the hemolyzed samples, thus decreasing the ^{23}Na NMR signals and bringing them to a level comparable to those obtained with intact cells. In hemolysates, the sodium concentrations determined by NMR were 94% of those measured by flame photometry. This may also be due to coagulation of the hemolysates, since this did not occur in water-diluted hemolysates in our study. Using erythrocytes with higher intracellular sodium concentrations, we measured a signal loss of greater amplitude than that observed by Yeh et al. (4). We suggest that the difference in the magnitude of the effect may be due to the poorer signal/noise ratio obtained in their studies as a result of the lower intracellular sodium concentration in human erythrocytes. In contrast, our results are compatible with those of a subsequent study on pig erythrocyte ghosts where the NMR signals were compared before and after addition of various amounts of sodium (5).

Two recent ^{23}Na NMR studies on human erythrocytes concluded that the totality of the intracellular sodium is NMR visible (8, 9). In both cases, a comparison was made between the measurements obtained by flame photometry and ^{23}Na NMR. Unfortunately, (*a*) these studies were not very exhaustive and some experimental parameters seem not to have been properly controlled; and (*b*) the intracellular aqueous volumes were not determined directly by isotope dilution. In one study (9), the hematocrit value of the samples was not taken into account. In both studies (8, 9) the variations of the hematocrit during the NMR experiment were not considered. These variations are not negligible since we measured a hematocrit change of 1% per minute under similar conditions. Due to these problems, it is not possible to compare the data reported in these publications with the data presented here.

Membrane Permeability to Dysprosium

The reported ^{23}Na and ^{39}K NMR studies on cell systems have assumed, on the basis of the good separation obtained between the intra- and extracellular signals, that the paramagnetic agent does not cross the cell membrane (7–11, 13–15). However, the downfield displacement of the intracellular ^{23}Na NMR resonance in erythrocytes (Figs. 1 and 2) suggests that a small quantity of free Dy^{3+} ion is incorporated into the cell. The displacement of chemical shift caused by the uncomplexed Dy^{3+} ion is in the opposite direction to that caused by the $Dy(PPP)_2^{7-}$ complex and its magnitude is approximately ten times smaller. We took advantage of this downfield shift for our NMR external standard (see Materials and Methods).

The presence of Dy^{+3} causes a drastic downfield shift and line broadening of the ^{31}P NMR resonances of all the phosphate metabolites in solution. Fig. 7 illustrates the changes observed in the ^{31}P NMR spectra of human erythrocytes that were incubated at 37°C with slow agitation in the presence of 5 mM $Dy(PPP)_2^{7-}$ for increasing periods of time. The bottom spectrum, which was acquired on a dysprosium-free suspension, displays sharp resonances corresponding (from left to right) to the 2- and 3-phosphates of diphosphoglycerate, to inorganic phosphate and to the γ-, α-, and β-phosphates of ATP (25). After 20 min of incubation, all the resonances were already broadened (Fig. 7 *b*) by dysprosium and this effect increased with time (Fig. 7 *b–e*) so that no ATP signal was observable after 19 h. The penetration of dysprosium into the cell is dependent upon the agitation and temperature. Little change in the spectra was observed after leaving the sample in the NMR magnet for at least 4 h at 37°C (no agitation). This is in agreement with a previous report (9).

To ascertain that the production of deoxyhemoglobin with time was not responsible for the broadening and shift of the phosphate signals, ^{31}P NMR spectra were compared on the same blood samples before and after deoxygenation

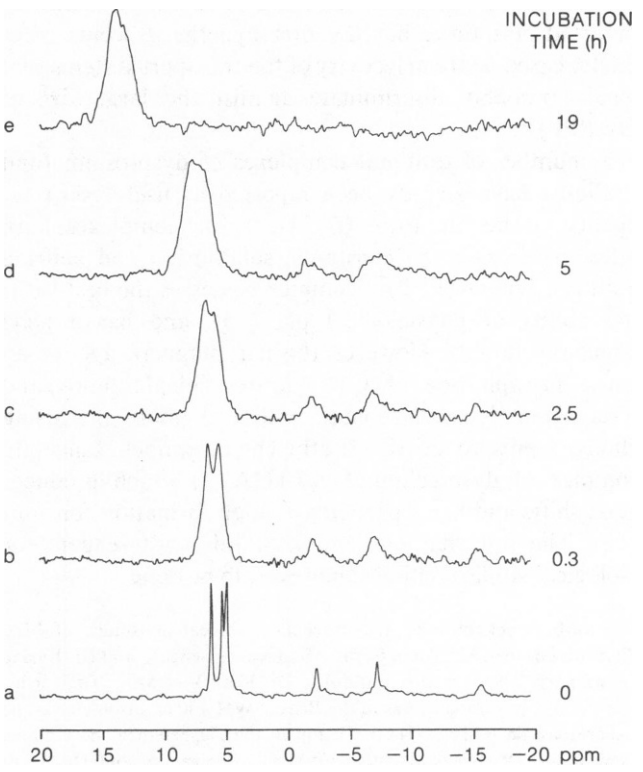

FIGURE 7 ^{31}P NMR spectra (162.0 MHz) of a human erythrocyte suspension after a pre-NMR incubation time of (*a*) 0, (*b*) 0.3, (*c*) 2.5, (*d*) 5, and (*e*) 19 h at 37°C with slow agitation. The composition of the suspension medium is given in Fig. 5. Spectra were acquired at 37°C using a 60 μs pulse length (90°), a spectral width of 10 kHz, a recycle time of 1.41 s and 1,000–2,000 accumulations.

by dithionite addition. No change in chemical shift was observable while a minor line broadening occurred. In contrast, Dy^{3+} had a drastic effect on both shift and line broadening of all observed phosphate-containing compounds (inorganic phosphate, phosphocreatine, adenosine triphosphate, adenosine diphosphate, adenosine monophosphate, 2-deoxyglucose-6-phosphate, and fructose-6-phosphate, results not shown).

The presence of small amounts of Dy^{3+} ion in cells does not affect the resolution of the ^{23}Na NMR signals from the two compartments, since the paramagnetic agent does not exist in the same form on both sides of the membrane, the shifting effect of the two forms being opposite. However, it is not known whether or not these ions will affect the metabolism of the cell. The biochemical integrity of the cell should, therefore, be verified before undertaking NMR investigations of this kind.

The accumulation of free Dy^{3+} ion into the cell can result from two processes. First, the $Dy(PPP)_2^{7-}$ complex can dissociate into free Dy^{3+} and tripolyphosphate ions and the Dy^{3+} moiety may enter the intracellular space. Although the dissociation constant for that process has, to our knowledge, not been reported, other workers believe the amount of free Dy^{3+} to be significant (14, 15). The other possibility is that the $Dy(PPP)_2^{7-}$ complex could enter the cell and be degraded by a cytoplasmic phosphatase. The distinction between these two possibilities cannot be made at this time, but the first hypothesis seems more likely, based on the selectivity of the transport systems that would probably discriminate against the large size of $Dy(PPP)_2^{7-}$.

A number of different complexes of dysprosium (and thulium) have already been reported as useful shift reagents in the literature (6–15). These complexes have different dissociation constants, solubilities, and shifting abilities. The $Dy(PPP)_2^{7-}$ complex possesses the best shifting ability at physiological pH (15), and has a good aqueous solubility. However, this paramagnetic agent may cause precipitation of Ca^{++} in physiologic fluids and Krebs-Henseleit bicarbonate buffer. A more promising choice seems to be the triethylenetetraminehexaacetate complex of dysprosium, $Dy(TTHA)^{3-}$, which produces good shifts and has a particularly high formation constant (15). The full characterization of this shift reagent for biological studies remains, however, to be done.

The authors acknowledge the excellent technical assistance of Mrs. Pierrette Fournel, Mr. Alain Cérat, Mr. Jacques Sénécal, and Dr. Binaye Soowamber. They are also grateful to Dr. Phan Viet Minh Tan for his help and for providing access to the Bruker WH 400 spectrometer in the Laboratoire de RMN à Haut Champ in the Département de Chimie. They thank Dr. Rhoda Blostein of McGill University and Dr. Jean-Claude Fouron of the Hôpital Ste-Justine for providing sheep blood.

The financial support of the Fondation Jean Michel (NMR time) and the Medical Research Council (MT 7875) are gratefully acknowledged. Y. Boulanger and P. Vinay are Chercheurs-Boursiers du Fonds de Recherche en Santé du Québec, and M. Desroches has a scholarship from the Fonds FCAC du Québec.

REFERENCES

1. Uldall, A., and A. Jensen. 1983. Determination of lithium, sodium and potassium in clinical chemistry. *In* Metal Ions in Biological Systems. H. Sigel, editor. Marcel Dekker, Inc., New York. 16:139–150.
2. Civan, M. M., and M. Shporer. 1978. NMR of sodium-23 and potassium-39 in biological systems. *In* Biological Magnetic Resonance. L. J. Berliner and J. Reuben, editors. Plenum Publishing Corp., New York. pp. 1–32.
3. Magnuson, J. A., and N. S. Magnuson. 1973. NMR studies of sodium and potassium in various biological tissues. *Ann. NY Acad. Sci.* 204:297–309.
4. Yeh, H. J. C., F. J. Brinley, Jr., and E. D. Becker. 1973. Nuclear magnetic resonance studies on intracellular sodium in human erythrocytes and frog muscle. *Biophys. J.* 13:56–71.
5. Monoi, H., and Y. Katsukura. 1976. Nuclear magnetic resonance of ^{23}Na in suspensions of pig erythrocyte ghosts: a comment on the interpretation of tissue ^{23}Na signals. *Biophys. J.* 16:979–981.
6. Pike, M. M., and C. S. Springer, Jr. 1982. Aqueous shift reagents for high-resolution cationic nuclear magnetic resonance. *J. Magn. Reson.* 46:348–353.
7. Gupta, R. K., and P. Gupta. 1982. Direct observation of resolved resonances from intra and extracellular sodium-23 ions in NMR studies of intact cells and tissues using dysprosium (III) tripolyphosphate as paramagnetic shift reagent. *J. Magn. Reson.* 47:344–350.
8. Pike, M. M., E. T. Fossel, T. W. Smith, and C. S. Springer, Jr. 1984. High resolution ^{23}Na NMR studies of human erythrocytes: use of aqueous shift reagents. *Am. J. Physiol.* 246:C528–C536.
9. Pettegrew, J. W., D. E. Woessner, N. J. Minshew, and T. Glonek. 1984. Sodium-23 NMR analysis of human whole blood, erythrocytes and plasma. Chemical shift, spin relaxation, and intracellular sodium concentration studies. *J. Magn. Reson.* 57:185–196.
10. Pike, M. M., S. R. Simon, J. A. Balschi, and C. S. Springer, Jr. 1982. High-resolution NMR studies of transmembrane cation transport: use of an aqueous shift reagent for ^{23}Na. *Proc. Natl. Acad. Sci. USA.* 79:810–814.
11. Balschi, J. A., V. P. Cirillo, and C. S. Springer, Jr. 1982. Direct high-resolution resonance studies of cation transport in vivo. Na^+ transport in yeast cells. *Biophys. J.* 38:323–326.
12. Pike, M. M., D. M. Yarmush, J. A. Balschi, K. E. Lenkinski, and C. S. Springer, Jr. 1983. Aqueous shift reagents for high-resolution cationic nuclear magnetic resonance. 2. ^{25}Mg, ^{39}K, and ^{23}Na resonances shifted by chelidamate complexes of dysprosium (III) and thulium (III). *Inorg. Chem.* 22:2388–2392.
13. Ogino, T., J. A. Den Hollander, and R. G. Shulman. 1983. ^{39}K, ^{23}Na, and ^{31}P NMR studies of ion transport in *Saccharomyces cerevisiae*. *Proc. Natl. Acad. Sci. USA.* 80:5185–5189.
14. Brophy, P. J., M. K. Hayer, and F. G. Riddell. 1983. Measurement of intracellular potassium ion concentrations by n.m.r. *Biochem. J.* 210:961–963.
15. Chu, S. C., M. M. Pike, E. T. Fossel, T. W. Smith, J. A. Balschi, and C. S. Springer, Jr. 1984. Aqueous shift reagents for high-resolution cationic nuclear magnetic resonance. III. $Dy(TTHA)^{3-}$, $Tm(TTHA)^{3-}$, and $Tm(PPP)_2^{7-}$. *J. Magn. Reson.* 56:33–47.
16. Kirk, R. G. 1977. Potassium transport and lipid composition in mammalian red blood cell membranes. *Biochim. Biophys. Acta.* 464:157–164.
17. Tosteson, D. C., and J. F. Hoffman. 1960. Regulation of cell volume by active cation transport in high and low potassium sheep red cells. *J. Gen. Physiol.* 44:169–194.
18. Parker, J. C. 1973. Dog red blood cells. Adjustment of density in vivo. *J. Gen. Physiol.* 61:146–157.
19. Giesbrecht, E., and L. F. Audrieth. 1958. Phosphates and polyphosphates of the rare earth elements. II. Pyrophosphato and triphosphato complexes of neodymium and yttrium. *J. Inorg. & Nucl. Chem.* 6:308–313.

20. Dunham, P. B., and R. Blostein. 1976. Active potassium transport in reticulocytes of high-K^+ and low-K^+ sheep. *Biochim. Biophys. Acta.* 455:749–758.

21. Inagaki, F., and T. Miyazawa. 1980. NMR analysis of molecular conformations and conformational equilibria with the lanthanide probe method. *Prog. Nucl. Magn. Reson. Spectrosc.* 14:67–111.

22. Brindle, K. M., F. F. Brown, I. D. Campbell, C. Grathwohl, and P. W. Kuchel. Application of spin-echo nuclear magnetic resonance to whole-cell systems. Membrane transport. *Biochem. J.* 180:37–44.

23. Venkatachalam, C. M., and D. W. Urry. 1980. Analysis of multisite ion binding using sodium-23 NMR with application to channel-forming micellar-packaged malonyl gramicidin. *J. Magn. Reson.* 41:313–335.

24. Forsēn, S., and B. Lindman. 1981. Ion binding in biological systems as studied by NMR spectroscopy. *Methods Biochem. Anal.* 27:289–486.

25. Marshall, W. E., A. J. R. Costello, T. O. Henderson, and A. Omachi. 1977. Organic phosphate binding to hemoglobin in intact human erythrocytes determined by ^{31}P nuclear magnetic resonance spectroscopy. *Biochim. Biophys. Acta.* 490:290–300.